

- 1 NEJM Original Article
- 2 2700 words. Current = 2638, including references and table/figure legends
- 3 5 Tables and Figures. Current = 3
- 4 40 references. Current = 24
- 5

32 **Abstract**

33 HCoV-19 (SARS-2) has caused >88,000 reported illnesses with a current case-fatality ratio of ~2%. Here,
34 we investigate the stability of viable HCoV-19 on surfaces and in aerosols in comparison with SARS-
35 CoV-1. Overall, stability is very similar between HCoV-19 and SARS-CoV-1. We found that viable virus
36 could be detected in aerosols up to 3 hours post aerosolization, up to 4 hours on copper, up to 24 hours on
37 cardboard and up to 2-3 days on plastic and stainless steel. HCoV-19 and SARS-CoV-1 exhibited similar
38 half-lives in aerosols, with median estimates around 2.7 hours. Both viruses show relatively long viability
39 on stainless steel and polypropylene compared to copper or cardboard: the median half-life estimate for
40 HCoV-19 is around 13 hours on steel and around 16 hours on polypropylene. Our results indicate that
41 aerosol and fomite transmission of HCoV-19 is plausible, as the virus can remain viable in aerosols for
42 multiple hours and on surfaces up to days.

43 A novel human coronavirus, now named severe acute respiratory syndrome coronavirus 2
44 (SARS-CoV-2, referred to as HCoV-19 throughout this manuscript) emerged in Wuhan, China in late
45 2019. As of March 3, 2020, >88,000 cases have been diagnosed in 64 countries, including 2915 deaths.¹
46 The rapid expansion of this outbreak is indicative of efficient human-to-human transmission.^{2,3} HCoV-19
47 has been detected in upper and lower respiratory tract samples from patients, with high viral loads in
48 upper respiratory tract samples.^{4,5} Therefore, virus transmission via respiratory secretions in the form of
49 droplets (>5 microns) or aerosols (<5 microns) appears to be likely. Virus stability in air and on surfaces
50 may directly affect virus transmission, as virus particles need to remain viable long enough after being
51 expelled from the host to be taken up by a novel host. Airborne transmission or fomite transmission were
52 thought to play important roles in the epidemiology of the two zoonotic coronaviruses that emerged this
53 century, SARS-CoV-1 and MERS-CoV.⁶ Airborne transmission may have been responsible for the largest
54 superspreading event during the SARS epidemic of 2002-2003,⁷ and numerous nosocomial
55 superspreading events of SARS-CoV-1 were linked to aerosol-generating medical procedures.⁸⁻¹⁰ Fomite
56 transmission was also suspected during the SARS epidemic, and one analysis of a nosocomial SARS-
57 CoV-1 superspreading event concluded that fomites had played a significant role.¹¹

58 Given the potential impact of different routes of transmission on the epidemiology of emerging
59 viruses, it is crucial to quantify the virological traits that may shape these aspects of HCoV-19
60 transmission. Here, we analyze the aerosol and surface stability of HCoV-19 and compare it with SARS-
61 CoV-1, the most closely related coronavirus known to infect humans.¹² We evaluated the aerosol stability
62 of HCoV-19 and SARS-CoV-1 for up to three hours in aerosols and up to 7 days on different surfaces.
63 We estimated decay rates of HCoV-19 and SARS-CoV-1 in each condition using a Bayesian regression
64 model.

65

66 **Methods**

67 HCoV-19 nCoV-WA1-2020 (MN985325.1)¹³ and SARS-CoV-1 Tor2 (AY274119.3)¹⁴ were the
68 strains used in our comparison. Virus stability in aerosols was determined as described previously at 65%

69 relative humidity (RH) and 21-23°C.¹⁵ In short, aerosols (<5 µm) containing HCoV-19 (10^{5.25}
70 TCID₅₀/mL) or SARS-CoV-1 (10^{6.75-7} TCID₅₀/mL) were generated using a 3-jet Collison nebulizer and
71 fed into a Goldberg drum to create an aerosolized environment. Aerosols were maintained in the
72 Goldberg drum and samples were collected at 0, 30, 60, 120 and 180 minutes post-aerosolization on a
73 47mm gelatin filter (Sartorius). Filters were dissolved in 10 mL of DMEM containing 10% FBS. Three
74 replicate experiments were performed.

75 Surface stability was evaluated on plastic (polypropylene, ePlastics), AISI 304 alloy stainless
76 steel (Metal Remnants), copper (99.9%) (Metal Remnants) and cardboard (local supplier) representing a
77 variety of household and hospital situations and was performed as described previously at 40% RH and
78 21-23°C using an inoculum of 10⁵ TCID₅₀/mL.¹⁶ This inoculum resulted in cycle-threshold values (Ct)
79 between 20 and 22 similar to those observed in samples from human upper and lower respiratory tract.⁴ In
80 short, 50 µl of virus was deposited on the surface and recovered at predefined time-points by adding 1 mL
81 of DMEM. Stability on cardboard was evaluated by depositing 50 µl of virus on the surface and
82 recovering the inoculum by swabbing of the surface, the swab was deposited 1 mL of DMEM. Three
83 replicate experiments were performed for each surface. Viable virus in all surface and aerosol samples
84 was quantified by end-point titration on Vero E6 cells as described previously.¹⁶ The Limit of Detection
85 (LOD) for the assays was 10^{0.5} TCID₅₀/mL for plastic, steel and cardboard and 10^{1.5} TCID₅₀/mL for copper
86 (due to toxicity caused by the copper in the undiluted samples).

87 The durations of detectability depend on initial inoculum and sampling method, as expected. To
88 evaluate the inherent stability of the viruses, we estimated the decay rates of viable virus titers using a
89 Bayesian regression model. This modeling approach allowed us to account for differences in initial
90 inoculum levels across replicates, as well as interval-censoring of titer data and other sources of
91 experimental noise. The model yields estimates of posterior distributions of viral decay rates and half-
92 lives in the various experimental conditions – that is, estimates of the range of plausible values for these
93 parameters given our data, with an estimate of the overall uncertainty.¹⁷ We describe our modeling
94 approach in more detail in the Supplemental Materials.

95

96 **Results**

97 HCoV-19 remained viable in aerosols throughout the duration of our experiment (180 minutes)
98 with a reduction in infectious titer 3 hours post-aerosolization from $10^{3.5}$ to $10^{2.7}$ CID_{50}/L (mean across
99 three replicates). This reduction in viable virus titer is relatively similar to the reduction observed in
100 aerosols containing SARS-CoV-1, from $10^{4.3}$ to $10^{3.5}$ $\text{TCID}_{50}/\text{mL}$ (mean across three replicates) (Figure
101 1A).

102 HCoV-19 was most stable on plastic and stainless steel and viable virus could be detected up to
103 72 hours post application (Figure 1B), though by then the virus titer was greatly reduced (polypropylene
104 from $10^{3.7}$ to $10^{0.6}$ $\text{TCID}_{50}/\text{mL}$ after 72 hours, stainless steel from $10^{3.7}$ to $10^{0.6}$ $\text{TCID}_{50}/\text{mL}$ after 48 hours,
105 mean across three replicates). SARS-CoV-1 had similar stability kinetics and live virus could be detected
106 on these surfaces up to 72 hours on polypropylene and 48 hours on stainless steel (polypropylene from
107 $10^{3.4}$ to $10^{0.7}$ $\text{TCID}_{50}/\text{mL}$ after 72 hours, stainless steel from $10^{3.6}$ to $10^{0.6}$ $\text{TCID}_{50}/\text{mL}$ after 48 hours, mean
108 across three replicates). No viable virus could be measured after 4 hours on copper for HCoV-19 and 8
109 hours for SARS-CoV-1, or after 24 hours on cardboard for HCoV-19 and 8 hours for SARS-CoV-1
110 (Figure 1B).

111 Both viruses exhibited exponential decay in viable virus titer across all experimental conditions,
112 as indicated by linear decrease in the $\log_{10}\text{TCID}_{50}/\text{mL}$ over time (Figure 2A). From the posterior
113 distributions on decay slope parameters we computed posterior distributions for the half-life of each virus
114 in each condition (Figure 2B, Table 1). HCoV-19 and SARS-CoV exhibited similar half-lives in aerosols,
115 with median estimates around 2.7 hours, and 95% credible intervals (2.5%–97.5% quantile range) of
116 (1.65, 7.24 hours) for HCoV-19 and (1.81, 5.45 hours) for SARS-CoV-1 (Table 1). Half-lives on copper
117 were also similar between the two viruses. On cardboard, HCoV-19 showed a considerably longer half-
118 life than SARS-CoV-1. Both viruses showed markedly longer viability on stainless steel and
119 polypropylene: the median half-life estimate for HCoV-19 was roughly 13 hours on steel and 16 hours on
120 polypropylene. In general, there was no statistically discernable difference in half-life between the two

121 viruses on any given surface except for cardboard: all other 95% credible intervals for the difference in
122 half-lives overlapped 0 (Fig 2B, Table 1).

123

124 **Discussion**

125 HCoV-19 has caused many more cases of illness and resulted in more deaths than SARS-CoV-1
126 and is proving more difficult to contain. Our results indicate that the greater transmissibility observed for
127 HCoV-19 is unlikely to be due to greater environmental viability of this virus compared to SARS-CoV-1.
128 Instead, there are a number of potential factors which could account for the epidemiological differences
129 between the two viruses. There have been early indications that individuals infected with HCoV-19 may
130 shed and transmit the virus while pre-symptomatic or asymptomatic^{4,18-20}. This reduces the efficacy of
131 quarantine and contact tracing as control measures relative to SARS-CoV-1.²¹ Other factors likely to play
132 a role include the infectious dose required to establish an infection, the stability of virus in mucus, and
133 environmental factors such as temperature and relative humidity.^{16,22} In ongoing experiments, we are
134 studying virus viability in different matrices, such as nasal secretion, sputum and fecal matter, and while
135 varying environmental conditions, such as temperature and relative humidity.

136 The epidemiology of SARS-CoV-1 was dominated by nosocomial transmission and SARS-CoV
137 was detected on variety of surfaces and objects in healthcare settings.⁹ HCoV-19 transmission is also
138 occurring in hospital settings, with over 3000 reported cases of hospital-acquired infections.²³ These cases
139 highlight the vulnerability of healthcare settings for introduction and spread of HCoV-19.¹⁰ However, in
140 contrast to SARS-CoV-1, most secondary transmission has been reported outside healthcare settings²³ and
141 widespread transmission in the community is being seen in several settings, such as households,
142 workplace and group gatherings.

143 A notable feature of SARS-CoV-1 was super-spreading events, in which a single infected
144 individual was responsible for a large number of secondary cases, well above the average number denoted
145 by the reproduction number R_{eff} .^{7-11,20} A tendency toward such super-spreading events has two important
146 consequences for the epidemiology of emerging infections: it makes any given introduction of infection

147 more likely to die out by chance, but when outbreaks do occur they are explosive and can overwhelm
148 hospital and public health capacity.²⁴ A number of hypothesized super-spreading events have been
149 reported for HCoV-19. Given that SARS-CoV-1 superspreading events were linked to aerosol and fomite
150 transmission,⁶⁻¹¹ our finding that HCoV-19 has viability in the environment comparable to that of SARS-
151 CoV-1 lends credence to the hypothesis that it too may be associated with superspreading.

152 We found that the half-life of HCoV-19 on cardboard is longer than the half-life of SARS-CoV-1.
153 It should be noted that individual replicate data were noticeably noisier for this surface than the other
154 surfaces tested (Figures S1–S5), so we advise caution in interpreting this result.

155 Here, we show that the stability of HCoV-19 and SARS-CoV-1 under the experimental
156 circumstances tested is similar. Taken together, our results indicate that aerosol and fomite transmission
157 of HCoV-19 are plausible, as the virus can remain viable in aerosols for multiple hours and on surfaces up
158 to days.

159

160 **Acknowledgements**

161 We would like to thank Kwe Claude Yinde and Michael Letko for experimental assistance. This research
162 was supported by the Intramural Research Program of the National Institute of Allergy and Infectious
163 Diseases (NIAID), National Institutes of Health (NIH). JOL-S and AG were supported by the Defense
164 Advanced Research Projects Agency DARPA PREEMPT # D18AC00031, and JOL-S was supported by
165 the U.S. National Science Foundation (DEB-1557022) and the Strategic Environmental Research and
166 Development Program (SERDP, RC□2635) of the U.S. Department of Defense. The findings and
167 conclusions in this report are those of the author(s) and do not necessarily represent the official position
168 of the Centers for Disease Control and Prevention. Names of specific vendors, manufacturers, or products
169 are included for public health and informational purposes; inclusion does not imply endorsement of the
170 vendors, manufacturers, or products by the Centers for Disease Control and Prevention or the US
171 Department of Health and Human Services.

172

173 **Code and data availability**

174 Code and data to reproduce the Bayesian estimation results and produce corresponding figures are

175 archived online at OSF: <insert link> and available on Github: <insert link>

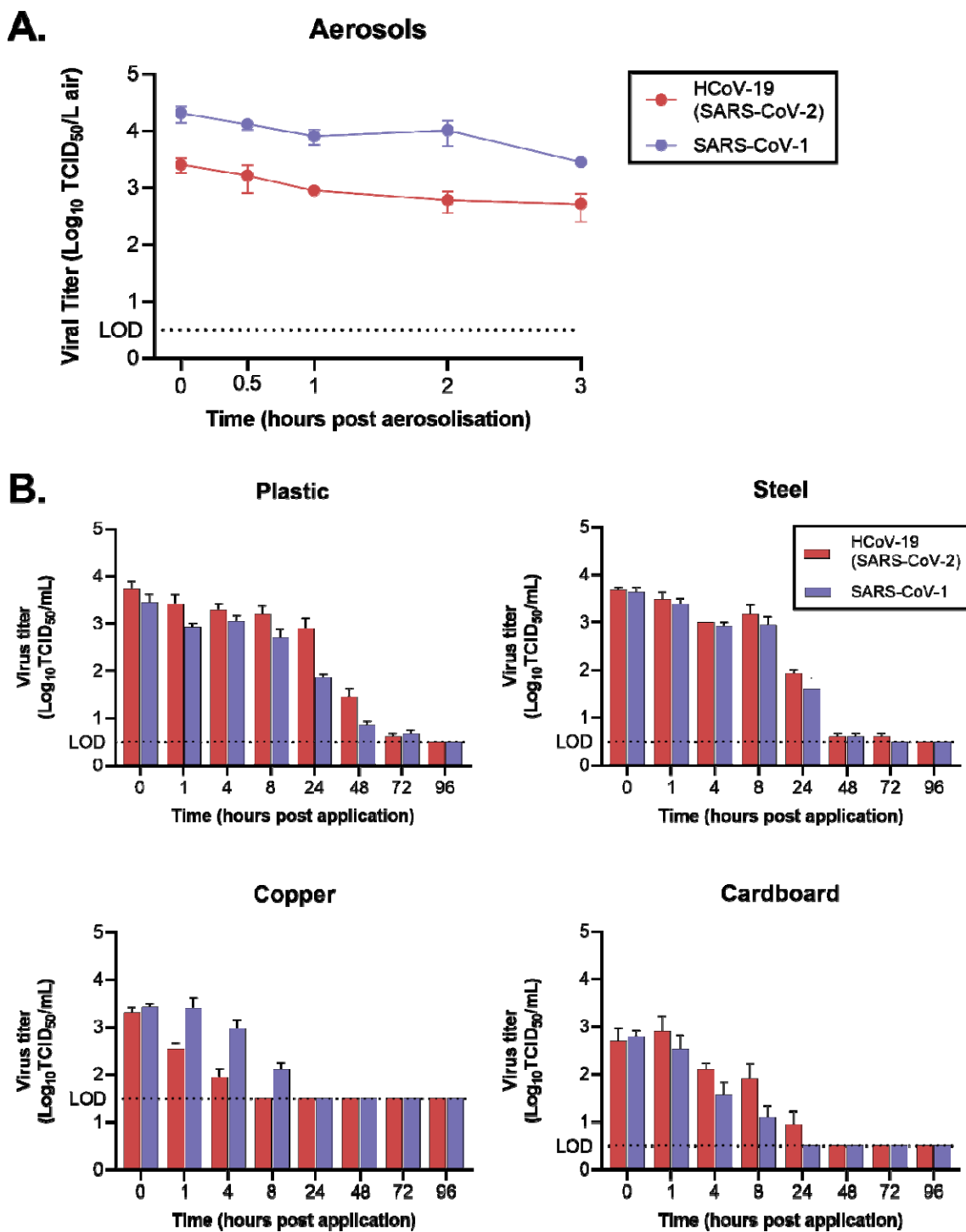
176

177

- 178 1. Coronavirus disease (COVID-2019) situation reports. 2020. (Accessed 26th of February 2020, at
179 <https://www.who.int/emergencies/diseases/novel-coronavirus-2019/situation-reports/>.)
- 180 2. Chan JF, Yuan S, Kok KH, et al. A familial cluster of pneumonia associated with the 2019 novel
181 coronavirus indicating person-to-person transmission: a study of a family cluster. *Lancet* 2020;395:514-
182 23.
- 183 3. Li Q, Guan X, Wu P, et al. Early Transmission Dynamics in Wuhan, China, of Novel Coronavirus-
184 Infected Pneumonia. *N Engl J Med* 2020.
- 185 4. Zou L, Ruan F, Huang M, et al. SARS-CoV-2 Viral Load in Upper Respiratory Specimens of
186 Infected Patients. *N Engl J Med* 2020.
- 187 5. Kim JY, Ko JH, Kim Y, et al. Viral Load Kinetics of SARS-CoV-2 Infection in First Two Patients in
188 Korea. *J Korean Med Sci* 2020;35:e86.
- 189 6. Otter JA, Donskey C, Yezli S, Douthwaite S, Goldenberg SD, Weber DJ. Transmission of SARS
190 and MERS coronaviruses and influenza virus in healthcare settings: the possible role of dry surface
191 contamination. *J Hosp Infect* 2016;92:235-50.
- 192 7. Yu IT, Li Y, Wong TW, et al. Evidence of airborne transmission of the severe acute respiratory
193 syndrome virus. *N Engl J Med* 2004;350:1731-9.
- 194 8. Christian MD, Loutfy M, McDonald LC, et al. Possible SARS coronavirus transmission during
195 cardiopulmonary resuscitation. *Emerg Infect Dis* 2004;10:287-93.
- 196 9. Chen YC, Huang LM, Chan CC, et al. SARS in hospital emergency room. *Emerg Infect Dis*
197 2004;10:782-8.
- 198 10. Judson SD, Munster VJ. Nosocomial Transmission of Emerging Viruses via Aerosol-Generating
199 Medical Procedures. *Viruses* 2019;11.
- 200 11. Xiao S, Li Y, Wong TW, Hui DSC. Role of fomites in SARS transmission during the largest
201 hospital outbreak in Hong Kong. *PLoS One* 2017;12:e0181558.
- 202 12. Wu A, Peng Y, Huang B, et al. Genome Composition and Divergence of the Novel Coronavirus
203 (2019-nCoV) Originating in China. *Cell Host Microbe* 2020.
- 204 13. Holshue ML, DeBolt C, Lindquist S, et al. First Case of 2019 Novel Coronavirus in the United
205 States. *N Engl J Med* 2020.
- 206 14. Marra MA, Jones SJ, Astell CR, et al. The Genome sequence of the SARS-associated
207 coronavirus. *Science* 2003;300:1399-404.
- 208 15. Fischer RJ, Bushmaker T, Judson S, Munster VJ. Comparison of the Aerosol Stability of 2 Strains
209 of Zaire ebolavirus From the 1976 and 2013 Outbreaks. *J Infect Dis* 2016;214:S290-S3.
- 210 16. van Doremalen N, Bushmaker T, Munster VJ. Stability of Middle East respiratory syndrome
211 coronavirus (MERS-CoV) under different environmental conditions. *Euro Surveill* 2013;18.
- 212 17. Gelman A. Bayesian data analysis. Third edition. ed. Boca Raton: CRC Press; 2014.
- 213 18. Bai Y, Yao L, Wei T, et al. Presumed Asymptomatic Carrier Transmission of COVID-19. *JAMA*
214 2020.
- 215 19. Rothe C, Schunk M, Sothmann P, et al. Transmission of 2019-nCoV Infection from an
216 Asymptomatic Contact in Germany. *N Engl J Med* 2020.
- 217 20. Tong ZD, Tang A, Li KF, et al. Potential Presymptomatic Transmission of SARS-CoV-2, Zhejiang
218 Province, China, 2020. *Emerg Infect Dis* 2020;26.
- 219 21. Munster VJ, Koopmans M, van Doremalen N, van Riel D, de Wit E. A Novel Coronavirus
220 Emerging in China - Key Questions for Impact Assessment. *N Engl J Med* 2020;382:692-4.
- 221 22. Lunn TJ, Restif O, Peel AJ, et al. Dose-response and transmission: the nexus between reservoir
222 hosts, environment and recipient hosts. *Philos Trans R Soc Lond B Biol Sci* 2019;374:20190016.

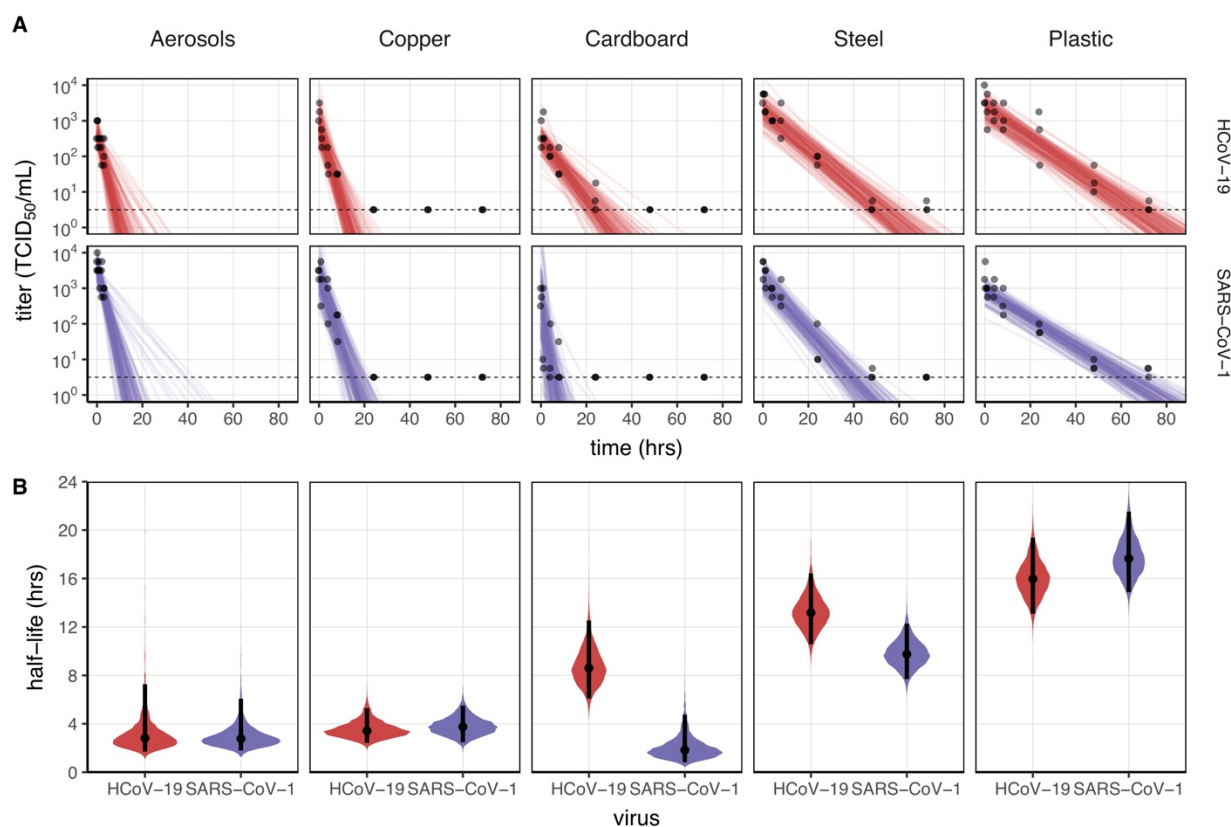
- 223 23. Wu Z, McGoogan JM. Characteristics of and Important Lessons From the Coronavirus Disease
224 2019 (COVID-19) Outbreak in China: Summary of a Report of 72314 Cases From the Chinese Center for
225 Disease Control and Prevention. JAMA 2020.
- 226 24. Lloyd-Smith JO, Schreiber SJ, Kopp PE, Getz WM. Superspreading and the effect of individual
227 variation on disease emergence. Nature 2005;438:355-9.

228



229
 230 Figure 1. Viability of SARS-CoV and HCoV-19 in aerosols and on different surfaces. A) SARS-CoV and
 231 HCoV-19 were aerosolized in a rotating drum maintained at 21-23°C and 65% RH. Aerosols were

232 maintained over 180 minutes and samples were collected at 0-, 30-, 60-, 120- and 180-minutes post
233 aerosolization. Viable virus titer per liter of air is shown in TCID₅₀/L air. B) 50 µl of 10⁵ TCID₅₀/mL of
234 SARS-CoV and HCoV-19 was applied on plastic, steel, copper and cardboard surfaces. At 1, 4, 8, 24, 48,
235 72, and 96 hours samples were obtained for viability assessment. All samples were quantified by end-
236 point titration on Vero E6 cells. Plots show the mean and standard error across three replicates. Dotted
237 line shows Limit of Detection (LOD), 10^{0.5} TCID₅₀/mL for plastic, steel and cardboard and 10^{1.5}
238 TCID₅₀/mL for copper.



239
240 Figure 2. Estimated exponential decay rates and corresponding half-lives for HCoV-19 and SARS-CoV-
241 1. Experimental conditions are ordered by posterior median half-life for HCoV-19. A: Regression plots
242 showing predicted decay of virus titer over time; titer plotted on a logarithmic scale. Points show
243 measured titers and are slightly jittered along the time axis to avoid overplotting. Lines are random draws
244 from the joint posterior distribution of the exponential decay rate (negative of the slope) and intercept
245 (initial virus titer), thus visualizing the range of possible decay patterns for each experimental condition.

246 150 lines per panel: 50 lines from each plotted replicate. Dotted line shows Limit of Detection (LOD),

247 $10^{0.5}$ TCID₅₀/mL. B: Violin plots showing posterior distribution for half-life of viable virus. Dot shows

248 the posterior median estimate and black line shows a 95% credible interval.

249

250 Table 1. Posterior median estimates and 95% credible intervals (2.5%–97.5% quantile range) for half-

251 lives of HCoV-19 and SARS-CoV in aerosols and on various surfaces, as well as a median estimate and

252 95% credible interval for the difference between the two half-lives (HCoV-19 – SARS-CoV).

253

<i>Material</i>	HCoV-19			SARS-CoV-1			HCoV-19 – SARS-CoV-1		
	<i>median</i>	2.5%	97.5%	<i>median</i>	2.5%	97.5%	<i>median</i>	2.5%	97.5%
Aerosols	2.74	1.65	7.24	2.74	1.81	5.45	-0.00418	-2.72	4.45
Copper	3.4	2.4	5.11	3.76	2.43	5.43	-0.321	-2.31	1.78
Cardboard	8.45	5.95	12.4	1.74	0.827	4.42	6.6	3.07	10.7
Steel	13.1	10.5	16.1	9.77	7.69	12.3	3.36	-0.173	7.12
Plastic	15.9	13	19.2	17.7	14.8	21.5	-1.79	-6.31	2.51

254